

¹ **MLS Aura HCl: Intercomparison and Historical** ² **Context**

D.J. Lary^{1,2}, O. Aulov^{1,2}

D.J. Lary, Goddard Earth Sciences and Technology Centre, University of Maryland Baltimore
County, Baltimore, MD 21228 (David.Lary@umbc.edu)

¹Goddard Earth Sciences and Technology
Centre, University of Maryland Baltimore
County, Baltimore, Maryland, USA

²Atmospheric Chemistry and Dynamics
Branch, NASA, Goddard Space Flight
Centre, Greenbelt, Maryland, USA

Abstract. We use probability distribution functions (PDFs) and scatter diagrams for validation and bias characterization of Aura Microwave Limb Sounder (MLS) HCl retrievals. Both these methods allow us to use large statistical samples and do not require correlative measurements to be co-located in space and time. The bias between the Halogen Occultation Experiment (HALOE) and Aura MLS is greatest above the 525 K (≈ 21 km) isentropic surface. The global average mean bias between Aura and the Atmospheric Chemistry Experiment (ACE) for January 2005 was 2.3% and between MLS Aura and HALOE was 13.9%. The global scatter diagram that compares all the contemporaneous observations of ACE and MLS Aura has a slope of 1.08. The global scatter diagram that compares all the contemporaneous observations of HALOE and MLS Aura has a slope of 0.91. The width of the PDFs are a measure of the spatial variability and measurement precision. The Aura MLS HCl PDFs are consistently wider than those for ACE and HALOE, this reflects the retrieval uncertainties. The median observation uncertainty for MLS Aura HCl is 12%, which is 50% larger than the median ACE v2.2 uncertainty of 8%. We also connect Aura MLS HCl with the heritage of HALOE HCl by using neural networks to learn the inter-instrument biases and provide a seamless HCl record from the launch of the Upper Atmosphere Research Satellite (UARS) in 1991 to the present.

1. Introduction

23 The Microwave Limb Sounder (MLS) on Aura is providing the first daily global ob-
24 servations of HCl [*Waters et al.*, 2006]. A preliminary validation of MLS HCl has been
25 presented by *Froidevaux et al.* [2006].

26 Satellite evaluation and validation are necessary, but sampling issues often make prac-
27 tical application problematic. In the traditional approach to validation, there is a com-
28 parison of matched pairs of profiles coincident in space and time. This strong constraint
29 dramatically reduces the statistical sample sizes we can deal with. The definition of ‘co-
30 incident’ observations varies, but 1000 km or more often separates such measurements.
31 While the approach is suitable for a quick comparison to establish that, the observations
32 are at least the correct order of magnitude, establishing instrument accuracy or precision
33 through such comparisons is difficult because of the limited number of coincident pairs
34 and the contribution of atmospheric variability. Furthermore, issues of representativeness
35 arise because the validation exercises are typically limited geographically. It is there-
36 fore useful to augment the traditional approach to validation with the use of probability
37 distribution functions (PDFs) of trace gases over an extended period for a given spatial
38 domain. In this study, we choose to form PDFs of an entire month of data and to specify
39 the spatial domain in terms of Lagrangian flow-tracking coordinates. The analysis starts
40 with the launch of UARS and continues up to the present. The scatter diagrams allow
41 us to compare a pair of instruments globally over the entire period of overlap using the
42 PDFs for each month, for each Lagrangian region.

43 PDFs have already been used in a variety of tracer studies [*Pierrehumbert*, 1994; *Yang*,
44 1995; *Sparling and Schoeberl*, 1995; *Rood et al.*, 2000; *Hu and Pierrehumbert*, 2001; *Gao*
45 *et al.*, 2002; *Johnson et al.*, 2002; *Strahan*, 2002; *Neu et al.*, 2003; *Hsu et al.*, 2004] and
46 in estimation of representativeness uncertainty in chemical data assimilation *Lary* [2003].

47 Not only does a PDF characterize the tracer distribution, its shape tells us about mix-
48 ing barriers, how complete the mixing is, and chemical processes such as ozone depletion
49 *Sparling* [2000]; *Pierrehumbert* [2000]; *Strahan* [2002]; *Neu et al.* [2003]. For example, a
50 narrow peak in the concentration PDF indicates that the air is well mixed and significant
51 variability generating processes have not recently occurred (e.g. long range transport). A
52 multi-modal distribution indicates air of different origins (e.g. polar and mid-latitude). In
53 general, broad peaks indicate recent variability generating processes such as photochem-
54 istry or transport (horizontal or vertical).

55 Measurement imprecision is one factor that affects the widths of the PDFs, and precision
56 of the measurements is certainly a parameter that needs validation. In many cases, this is
57 difficult because atmospheric variability swamps the effects of measurement imprecision.
58 The PDF plots of the type described here might also help to reduce the atmospheric
59 variability by indicating locations and conditions where it is minimized. Comparisons
60 between measurements under these conditions can be used to produce upper limits on
61 measurement imprecision.

62 Because a major component of the variability of trace gases is due to atmospheric
63 transport we make our comparisons in equivalent PV latitude - potential temperature
64 coordinates [*Schoeberl et al.*, 1989; *Proffitt et al.*, 1989; *Lait et al.*, 1990; *Douglass et al.*,

1990; *Lary et al.*, 1995; *Schoeberl et al.*, 2000]. Using these coordinates also extends the effective latitudinal coverage of the measurements.

Section 2 describes the HCl intercomparison using PDFs and scatter diagrams and the cross-calibration of HCl retrievals using neural networks. Section 3 presents a continuous time-series of HCl from the launch of UARS to the present. Section 4 gives a summary.

2. HCl Intercomparison

We compare measurements of HCl from the different instruments in Table 1. Table 1 also gives the median observation uncertainty over the entire record of each instrument. The Halogen Occultation Experiment (HALOE) provides the longest record of space based HCl observations. Aura MLS has a vertical resolution which is 3 km in the lower stratosphere increasing to 5-6 km near 1 hPa and 7 km near 0.22 hPa. ACE has a vertical resolution of about 4 km from the cloud tops to about 150 km. The ACE and HALOE retrievals are given on a much finer altitude grid, with a spacing of 1 km or less. The MLS Aura retrievals used are given on an altitude grid with a spacing of ≈ 2.5 km.

2.1. PDFs

Figure 1 show example HCl PDFs for the three instruments HALOE, ACE and MLS Aura. In each case the PDFs are for all observations made by that instrument in a Lagrangian region for three isentropic levels centered on an equivalent latitude of 55°N during all the Januarys that the instruments observed (panels a to c) or for the observations made only during January 2005 (panels d to f). A consistent picture is seen in these plots: Aura MLS agrees very well with ACE, while HALOE HCl retrievals are lower than those from the other instruments. There is a general increase in the bias with increasing

85 altitude, particularly noticeable at the 525 K (≈ 21 km) surface and above. Previous
 86 comparisons among HCl datasets reveal a similar bias for HALOE [*Russell et al.*, 1996;
 87 *McHugh et al.*, 2005; *Froidevaux et al.*, 2006].

2.2. Width of the PDFs

The width of the PDFs, σ_{rep} , gives us a measure of the spatial variability (representative-
 ness) in the tracer field [*Lary*, 2003]. A robust estimator of the width of the distribution
 is the average deviation [*Press et al.*, 1992],

$$\sigma_{rep} = ADev(\chi_1 \dots \chi_N) = \frac{1}{N} \sum_{j=1}^N |\chi_j - \bar{\chi}| \quad (1)$$

88 where χ is the tracer volume mixing ratio (v.m.r.), and the over-bar indicates the mean
 89 of the N observations considered. It is interesting to look at a cross-section of the repre-
 90 sentativeness as it highlights the regions with large gradients. Figure 2 shows the PDF
 91 width for HCl observations made by Aura MLS during January 2005. The up-welling air
 92 over the tropics is visible as is the large spatial variability in the lower stratospheric polar
 93 vortex at high northern latitudes.

94 The width of the PDF could be characterized in several ways. Two other common
 95 measures are the variance, or its square root, the standard deviation. Both of these
 96 measures have been tried and give essentially the same results. The reason for choosing
 97 the average deviation is that the variance and standard deviation depend on the second
 98 moment of the PDF. It is not uncommon to have a distribution whose second moment
 99 does not exist (i.e., is infinite). In this case, the variance or standard deviation is useless
 100 as a measure of the data's width about a central value. This can occur even when the

101 width of the peak looks, by eye, perfectly finite. The average deviation is a more robust
102 estimator that does not suffer from this problem [*Press et al.*, 1992].

103 Even though the median values of the Aura MLS and ACE PDFs are very similar,
104 the width of the Aura MLS HCl PDFs are consistently larger than those for ACE and
105 HALOE, this reflects the retrieval uncertainties shown in Table 1. The median observation
106 uncertainty for MLS Aura HCl is 12%, which is 50% larger than the median ACE v2.2
107 uncertainty of 8%. However, the instruments generally have a similar spatial distribution,
108 e.g. both Aura MLS and ACE have wide PDFs the lower stratosphere vortex, and narrow
109 PDFs in the upper stratosphere. Likewise, the HALOE PDFs for a given month, are
110 narrower than the ACE PDFs and the median HALOE uncertainty is less than median
111 ACE observation uncertainty (e.g. Figure 1 panels a to c).

2.3. Biases

112 We can take the difference between the medians of the PDFs as a measure of the inter-
113 instrument bias. This bias is really only significant if it is larger than the atmospheric
114 variability in the Lagrangian region we are considering.

115 Figure 3 shows inter-instrument biases for January 2005 for Aura, ACE and HALOE.
116 The left hand panels show the bias as a volume-mixing ratio (v.m.r.). The right hand
117 panels show the percentage bias. Panels (a) to (d) are for the biases between ACE v2.2
118 and Aura MLS v01. In panels (a) and (b) we show all available Lagrangian regions were
119 both ACE and Aura made observations during January 2005. In Panels (c) and (d) we
120 only plot Lagrangian regions where the bias was greater than the natural HCl variability
121 in that region of the atmosphere, we have called this the useful bias.

122 We note that for the January 2005 example, the bias between Aura and ACE in the
123 lower stratosphere is less than the natural variability. The average mean bias between
124 Aura and ACE for January 2005 was 2.3%. Figure 3 (e) and (f) show the analogous bias
125 for HALOE and Aura, only those Lagrangian regions where the bias was greater than the
126 natural HCl variability have been plotted. We note that for the January 2005 example,
127 the bias between HALOE and Aura is greater than the natural variability throughout
128 most of the stratosphere. The average mean bias between Aura and HALOE for January
129 2005 was 13.9%.

2.4. Scatter Diagrams and Cross Calibration

130 So far, we have compared the PDFs for all overlapping Lagrangian regions for a given
131 month. However, we can use a single scatter diagram to compare all the overlaps glob-
132 ally for all the months observed by each pair of instruments. Such a scatter diagram
133 has the advantage of a huge sample size, it encompasses the entire period that a pair
134 of instruments were making contemporaneous observations. Figure 4 shows two scat-
135 ter diagrams for all the contemporaneous observations of HCl made by globally by two
136 pairs of instruments. In panel (a) we compare ACE and MLS Aura which were making
137 contemporaneous observations between January 2004 and November 2005. In panel (b)
138 we compare HALOE and MLS Aura which were making contemporaneous observations
139 between September 2004 and November 2005.

140 In the ideal case where we have perfect agreement between two instruments, the slope
141 of the scatter diagram would be 1 and the intercept would be 0. In the case of ACE and
142 Aura, we see there is a slope of 1.08, and for HALOE Aura there is a slope of 0.91. We
143 also note that in the case of MLS Aura and HALOE, the scatter diagrams do not have

144 a constant slope over the entire range of HCl values, several ‘wiggles’ are present. This
145 means that the inter-instrument biases are spatially and temporally dependent. Neural
146 networks are multi-variate, non-parametric, ‘learning’ algorithms that are ideally suited
147 to learning, and correcting for, such inter-instrument biases.

148 We have used a neural network with three inputs and one output. The inputs are
149 equivalent PV latitude, potential temperature, and HCl from instrument A. The output
150 is HCl from instrument B. The neural network algorithm used was a feed-forward back-
151 propagation network with 20 hidden nodes. The training was done by the Levenberg-
152 Marquardt back-propagation algorithm provided by the Matlab neural network toolbox
153 (<http://www.mathworks.com/products/neuralnet/>).

154 The panels on the left of Figure 5 shows the results of such a neural-network training
155 to learn inter-instrument biases between ACE v2.2, Aura MLS v1 and HALOE v19 HCl.
156 The panels on the right of Figure 5 show an independent validation of the training using
157 a randomly chosen, totally independent, data sample *not* used in training the neural
158 network. In each case the x-axis shows the actual ACE v2.2 HCl (the target). In panels
159 (a) and (b) the y-axis is the neural network estimate of ACE v2.2 HCl based on MLS
160 Aura v01 HCl. Panel (a) shows the results using the training data, panel (b) shows
161 the results of the independent validation. In panels (c) and (d) the y-axis is the neural
162 network estimate of ACE v2.2 HCl based on HALOE v19 HCl. Panel (c) shows the results
163 using the training data, panel (d) shows the results of the independent validation. The
164 mapping has removed the bias between the measurements and has also straightened out
165 the ‘wiggles’ seen in Figure 4.

3. HCl Timeseries

166 Now that we have completely characterized the inter-instrument biases and been able to
167 correct for them we can connect Aura MLS HCl observations to the heritage of HALOE.
168 This allows us to produce an HCl time-series from the launch of UARS in 1991 up-to the
169 present. Figure 6 shows such an HCl time-series for 55°N for three isentropic levels (525 K
170 \approx 21 km, 800 K \approx 30 km, 1300 K \approx 41 km) from the launch of UARS to the present with
171 HCl observations from HALOE, ATMOS, CRISTA, ACE, MkIV and Aura MLS.

172 The panels on the left use the original v19 HALOE data, and the low bias of HALOE
173 HCl relative to all other instruments is evident. The panels on the right use the HALOE
174 v19 data re-calibrated with a neural network to agree with ACE v2.2 HCl. If we compare
175 the left and right panels we see that, as expected, the re-calibration brings the HALOE
176 data into good agreement with ACE and Aura MLS data, and the *independent* ATMOS
177 HCl data.

178 We also performed a re-calibration of the ACE and MLS data to agree with HALOE
179 v19. These two HCl re-calibrations have been used by *Lary et al.* [2006] to form a long
180 Cl_y time-series and associated uncertainty estimate (typically ≤ 0.4 ppbv at 800 K). The
181 uncertainty in the Cl_y estimate is primarily due to the discrepancy between the different
182 observations of HCl, i.e. the HALOE, Aura MLS, and ACE inter-instrument biases.

4. Summary

183 We have used PDFs to characterize the inter-instrument biases between the HCl prod-
184 ucts provided by Aura MLS v01, ACE v2.2, and HALOE v19. These biases are pre-
185 sented in a number of ways. First, as global equivalent latitude potential tempera-

186 ture cross-sections for every month of overlap between the instruments (available from
187 <http://www.pdfcentral.info/>).

188 The bias between HALOE and Aura MLS is greatest above the 525 K (≈ 21 km) isen-
189 tropic surface. The global average mean bias between Aura and ACE for January 2005
190 was 2.3% and between Aura and HALOE was 13.9%. Second, as global scatter diagrams.
191 A single scatter diagram compares all the overlaps globally for all the months observed
192 by each pair of instruments. In the case of ACE and Aura, we see there is a slope of 1.08,
193 and for HALOE Aura there is a slope of 0.91.

194 The width of the PDFs are a measure of the spatial variability. The Aura MLS HCl
195 PDFs are consistently larger than those for ACE and HALOE, this reflects the retrieval
196 uncertainties. The median observation uncertainty for MLS Aura HCl is 12%, which is
197 50% larger than the median ACE v2.2 uncertainty of 8%. The instruments generally have
198 a similar spatial distribution, e.g. both Aura MLS and ACE have wide PDFs the lower
199 stratosphere vortex, and narrow PDFs in the upper stratosphere.

200 We used neural networks to correct for inter-instrument biases and produce a con-
201 sistent time series of HCl from 1991 to the present. Such an HCl time-series is of
202 use in estimating a time-series of Cl_y . The HCl time-series are available in the elec-
203 tronic supplement. All of the standard and re-calibrated retrievals used in this study
204 to form the PDFs are available in a uniform format from [http://www.autochem.info/](http://www.autochem.info/constituentobservationaldatabase.html)
205 [constituentobservationaldatabase.html](http://www.autochem.info/constituentobservationaldatabase.html).

206 **Acknowledgments.** It is a pleasure to acknowledge NASA for research funding, Lu-
207 cien Froidevaux and the Aura MLS team for their data, the ACE team, Peter Bernath,
208 Chris Boone, and Kaley Walker for their data, the HALOE team and Ellis Remsberg for

209 their data, the ATMOS team for their data, the MkIV team for their data, Bill Read,
210 Anne Douglass, Rich Stolarski and Paul Newman for numerous useful conversations.

References

- 211 Bernath, P. F., et al., Atmospheric chemistry experiment (ace): Mission overview, *Geo-*
212 *phys. Res. Lett.*, *32*(15), 115S01, 2005.
- 213 Douglass, A., R. Rood, R. Stolarski, M. Schoeberl, M. Proffitt, J. Margitan, M. Loewen-
214 stein, J. Podolske, and S. Strahan, Global 3-dimensional constituent fields derived from
215 profile data, *Geophys. Res. Lett.*, *17*(4 SS), 525–528, 1990.
- 216 Froidevaux, L., et al., Early validation analyses of atmospheric profiles from EOS MLS
217 on the aura satellite, *IEEE Trans. Geosci. Remote Sens.*, *44*(5), 1106–1121, 2006.
- 218 Gao, R. S., et al., Role of noy as a diagnostic of small-scale mixing in a denitrified polar
219 vortex, *J. Geophys. Res. (Atmos.)*, *107*(D24), 2002.
- 220 Hsu, J., M. J. Prather, O. Wild, J. K. Sundet, I. S. A. Isaksen, E. V. Browell, M. A.
221 Avery, and G. W. Sachse, Are the trace-p measurements representative of the western
222 pacific during march 2001?, *J. Geophys. Res. (Atmos.)*, *109*(D2), 2004.
- 223 Hu, Y., and R. T. Pierrehumbert, The advection-diffusion problem for stratospheric flow.
224 part i: Concentration probability distribution function, *J. Atmos. Sci.*, *58*(12), 1493–
225 1510, 2001.
- 226 Johnson, D. R., A. J. Lenzen, T. H. Zapotocny, and T. K. Schaack, Numerical uncertain-
227 ties in simulation of reversible isentropic processes and entropy conservation: Part II,
228 *J. Clim.*, *15*(14), 1777–1804, 2002.
- 229 Lait, L., et al., Reconstruction of O₃ and N₂O fields from ER-2, DC-8, and balloon obser-
230 vations, *Geophys. Res. Lett.*, *17*(4 SS), 521–524, 1990.
- 231 Lary, D., Representativeness uncertainty in chemical data assimilation highlight mixing
232 barriers, *Atmos. Sci. Lett.*, *5*(1-4), 35–41, 2003.

- 233 Lary, D., M. Chipperfield, J. Pyle, W. Norton, and L. Riishojgaard, 3-dimensional
234 tracer initialization and general diagnostics using equivalent PV latitude-potential-
235 temperature coordinates, *Q. J. R. Meteorol. Soc.*, *121*(521 PtA), 187–210, 1995.
- 236 Lary, D. J., D. W. Waugh, A. R. Douglass, R. S. Stolarski, P. A. Newman, and M. Mussa,
237 Variations in stratospheric inorganic chlorine between 1991 and 2006, *Geophys. Res.*
238 *Lett.*, *submitted*, 2006.
- 239 McHugh, M., B. Magill, K. A. Walker, C. D. Boone, P. F. Bernath, and J. M. Russell,
240 Comparison of atmospheric retrievals from ace and haloe, *Geophys. Res. Lett.*, *32*(15),
241 0094-8276 L15S10, 2005.
- 242 Neu, J. L., L. C. Sparling, and R. A. Plumb, Variability of the subtropical "edges" in the
243 stratosphere, *J. Geophys. Res. (Atmos.)*, *108*(D15), 2003.
- 244 Pierrehumbert, R. T., Tracer microstructure in the large-eddy dominated regime, *Chaos*
245 *Solitons & Fractals*, *4*(6), 1091–1110, 1994.
- 246 Pierrehumbert, R. T., Lattice models of advection-diffusion, *Chaos*, *10*(1), 61–74, 2000.
- 247 Press, W., S. Teukolsky, W. Vetterling, and B. Flannery, *Numerical Recipes in Fortran -*
248 *The Art of Scientific Computing*, 2nd ed., Cambridge Univ. Press, New York, 1992.
- 249 Proffitt, M., et al., Insitu ozone measurements within the 1987 antarctic ozone hole from a
250 high-altitude ER-2 aircraft, *J. Geophys. Res. (Atmos.)*, *94*(D14), 16,547–16,555, 1989.
- 251 Rood, R. B., A. R. Douglass, M. C. Cerniglia, L. C. Sparling, and J. E. Nielsen, Sea-
252 sonal variability of middle-latitude ozone in the lowermost stratosphere derived from
253 probability distribution functions, *J. Geophys. Res. (Atmos.)*, *105*(D14), 17,793–17,805,
254 2000.

- 255 Russell, J. M., et al., The Halogen Occultation Experiment, *J. Geophys. Res. (Atmos.)*,
256 98(D6), 10,777–10,797, 1993.
- 257 Russell, J. M., et al., Validation of hydrogen chloride measurements made by the halogen
258 occultation experiment from the UARS platform, *J. Geophys. Res. (Atmos.)*, 101(D6),
259 10,151–10,162, 0148-0227, 1996.
- 260 Schoeberl, M. R., L. C. Sparling, C. H. Jackman, and E. L. Fleming, A lagrangian view of
261 stratospheric trace gas distributions, *J. Geophys. Res. (Atmos.)*, 105(D1), 1537–1552,
262 2000.
- 263 Schoeberl, M. R., et al., Reconstruction of the constituent distribution and trends in
264 the antarctic polar vortex from er-2 flight observations, *J. Geophys. Res. (Atmos.)*,
265 94(D14), 16,815–16,845, 1989.
- 266 Sparling, L. C., Statistical perspectives on stratospheric transport, *Rev. Geophys.*, 38(3),
267 417–436, 2000.
- 268 Sparling, L. C., and M. R. Schoeberl, Mixing entropy analysis of dispersal of aircraft
269 emissions in the lower stratosphere, *J. Geophys. Res. (Atmos.)*, 100(D8), 16,805–16,812,
270 1995.
- 271 Strahan, S., Influence of planetary wave transport on arctic ozone as observed by polar
272 ozone and aerosol measurement (poam) iii, *J. Geophys. Res. (Atmos.)*, 107(D20), 2002.
- 273 Waters, J. W., et al., The earth observing system microwave limb sounder (eos mls) on
274 the aura satellite, *IEEE Trans. Geosci. Remote Sens.*, 44(5), 1075–1092, 2006.
- 275 Yang, H. J., 3-dimensional transport of the ertel potential vorticity and N₂O in the GFDL
276 skyhi model, *J. Atmos. Sci.*, 52(9), 1513–1528, 1995.

277 Zander, R., M. R. Gunson, C. B. Farmer, C. P. Rinsland, F. W. Irion, and E. Mahieu, The
278 1985 chlorine and fluorine inventories in the stratosphere based on atmos observations
279 at 30-degrees north latitude, *J. Atmos. Chem.*, 15(2), 171–186, 1992.

Instrument	Temporal Coverage	Reference	Median Observation Uncertainty
ACE	2004-2006	<i>Bernath et al.</i> [2005]	8%
ATMOS	1991, 1993, 1994	<i>Zander et al.</i> [1992]	8%
Aura MLS	2004-2006	<i>Froidevaux et al.</i> [2006]	12%
HALOE	1991-2005	<i>Russell et al.</i> [1993]	4%

Table 1. The instruments used in this study. The uncertainties given are the median uncertainties of the level 2 product for all the observations made.

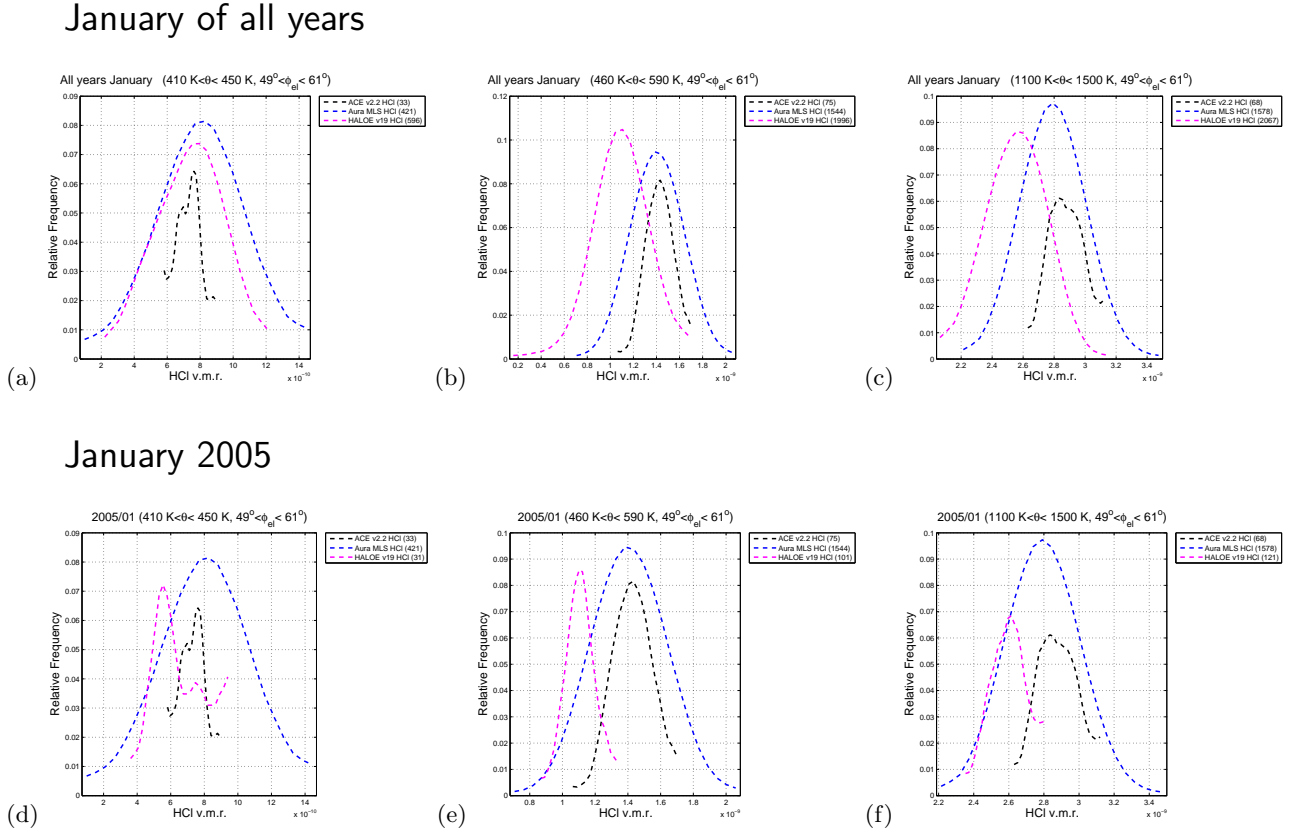


Figure 1. Panels (a) to (c) show example HCl PDFs for the three instruments HALOE, ACE and MLS Aura. In each case the PDFs are for all observations made by that instrument in a Lagrangian region for three isentropic levels centered on an equivalent latitude of 55°N during all the January's that the instrument observed. For panel (a) we plot a PDF for all observations in the range $410\text{ K} < \theta < 450\text{ K}$, $49^\circ < \phi_{el} < 61^\circ$. For panel (b) we plot a PDF for all observations in the range $460\text{ K} < \theta < 590\text{ K}$, $49^\circ < \phi_{el} < 61^\circ$. For panel (c) we plot a PDF for all observations in the range $1100\text{ K} < \theta < 1500\text{ K}$, $49^\circ < \phi_{el} < 61^\circ$. Panels (d) to (f) are analogous to (a) to (c) for the observations made only during January 2005. The number of observations used to form each PDF is shown in parenthesis in the legend. The plots in panels (a) to (c) are available online at http://www.pdfcentral.info/HCl/all/01/all.01_nh.html and for panels (d) to (f) at http://www.pdfcentral.info/HCl/2005/01/2005.01_nh.html

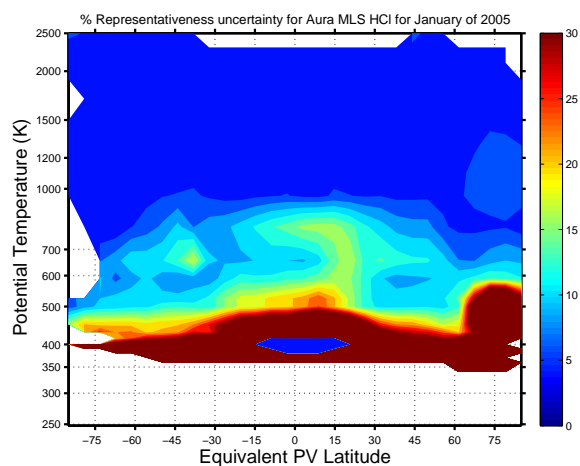


Figure 2. This figure shows the PDF width characterized by the average deviation for HCl observations made by Aura MLS during January 2005. The width of the PDFs, σ_{rep} , gives us a measure of the spatial variability (representativeness) in the tracer field and highlights the regions with large spatial gradients. This plot is available online at http://www.pdfcentral.info/HCl/2005/01/2005_01_clim.html.

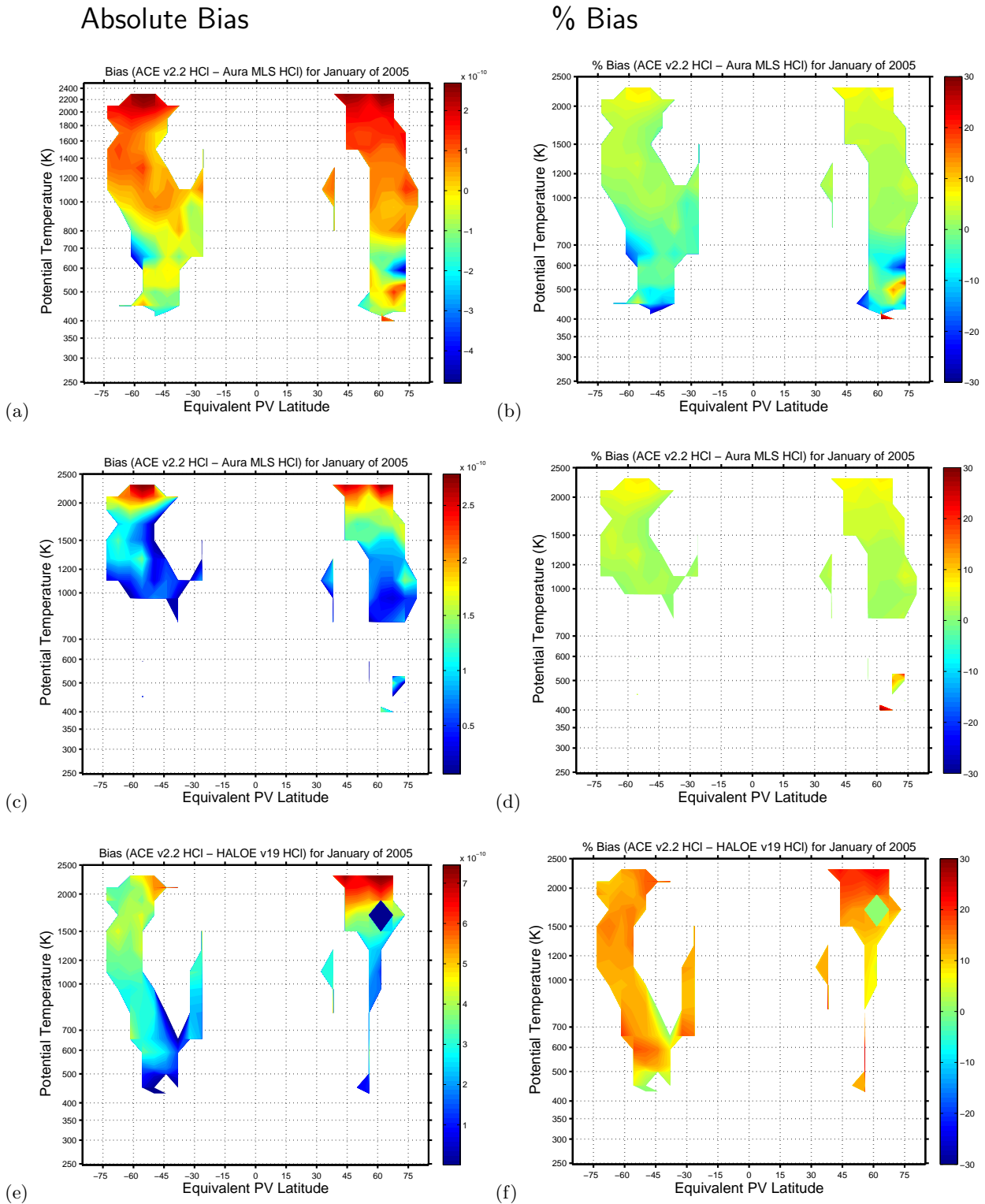


Figure 3. The panels show inter-instrument biases for January 2005. These biases are the differences in the PDF medians for each instrument. The left hand panels show the bias as a volume-mixing ratio (v.m.r.). The right hand panels show the percentage bias. The bias is only significant if it is greater than the natural variability in that region of the atmosphere. The natural variability (representativeness) has been diagnosed by taking the width of the PDF as measured by the average deviation of the PDF. Panels (a) to (d) are for the biases between ACE v2.2 and Aura MLS v01. In panels (a) and (b) we show all available Lagrangian regions where both ACE and Aura made observations during January 2005. In Panels (c) and (d) we only plot Lagrangian regions where the bias was greater than the natural HCl variability in that region of the atmosphere, we have called this the useful bias. It can be seen that for most of the Lagrangian regions observed by both ACE and Aura the bias is less than 10%. Panels (e) and (f) show the analogous bias for HALOE and Aura where the bias was greater than the natural HCl variability. The plots are available online at http://www.pdfcentral.info/HCl/2005/01/2005_01_bias.html.

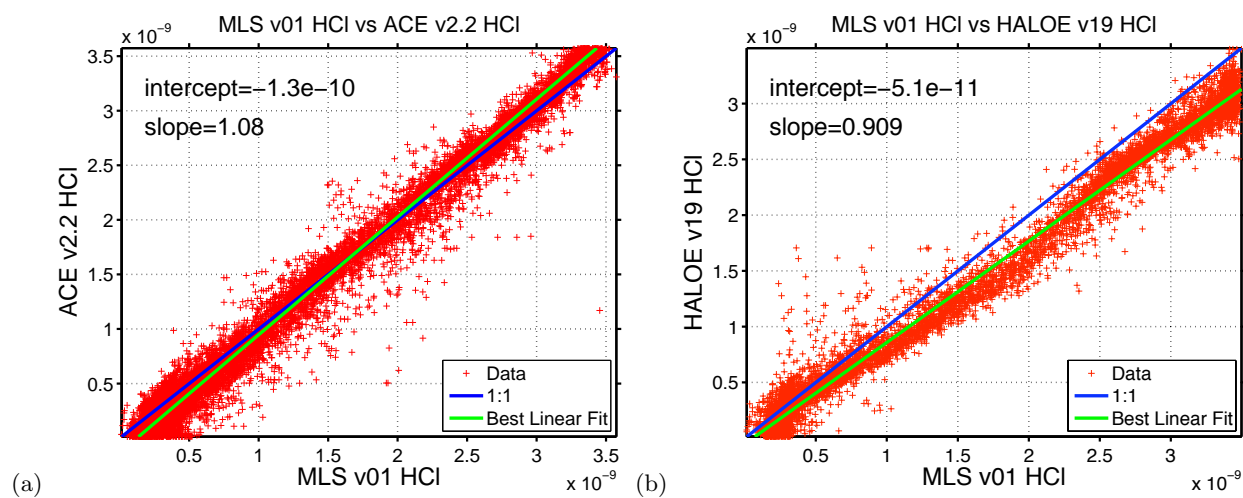
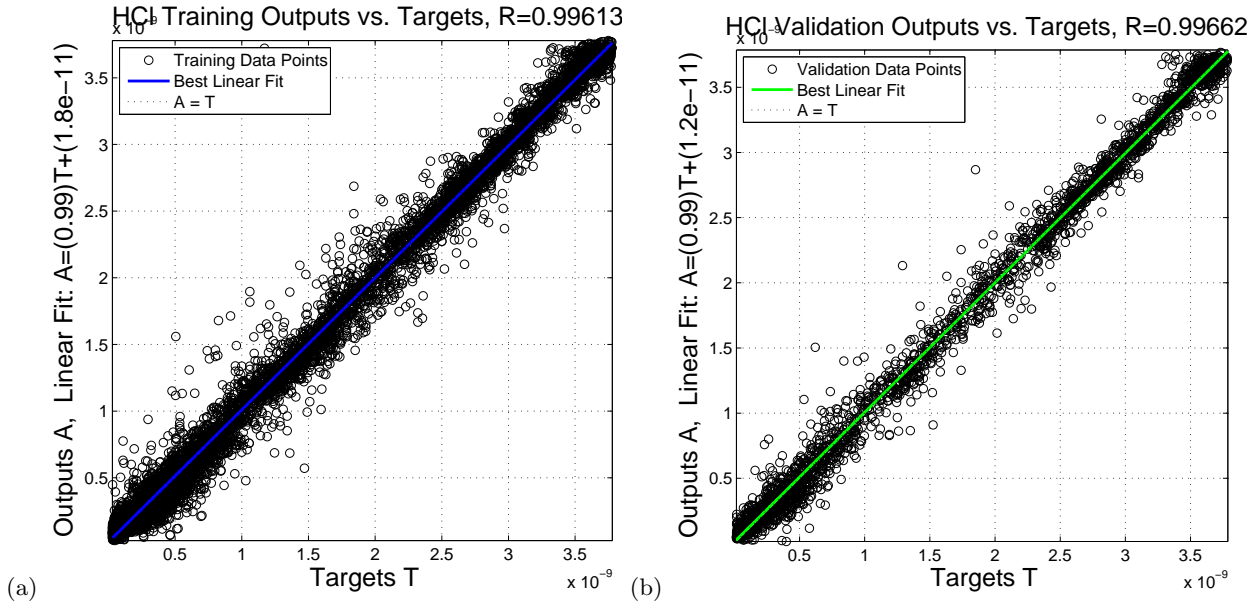


Figure 4. Panels (a) and (b) show scatter plots of all contemporaneous observations of HCl made by HALOE, ACE and MLS Aura. Each point plotted is the median value of a PDF of observations made for a Lagrangian region over the period of a month.

Training

Independent Validation

Recalibrating MLS Aura HCl to agree with ACE v2.2 HCl



Recalibrating HALOE v19 HCl to agree with ACE v2.2 HCl

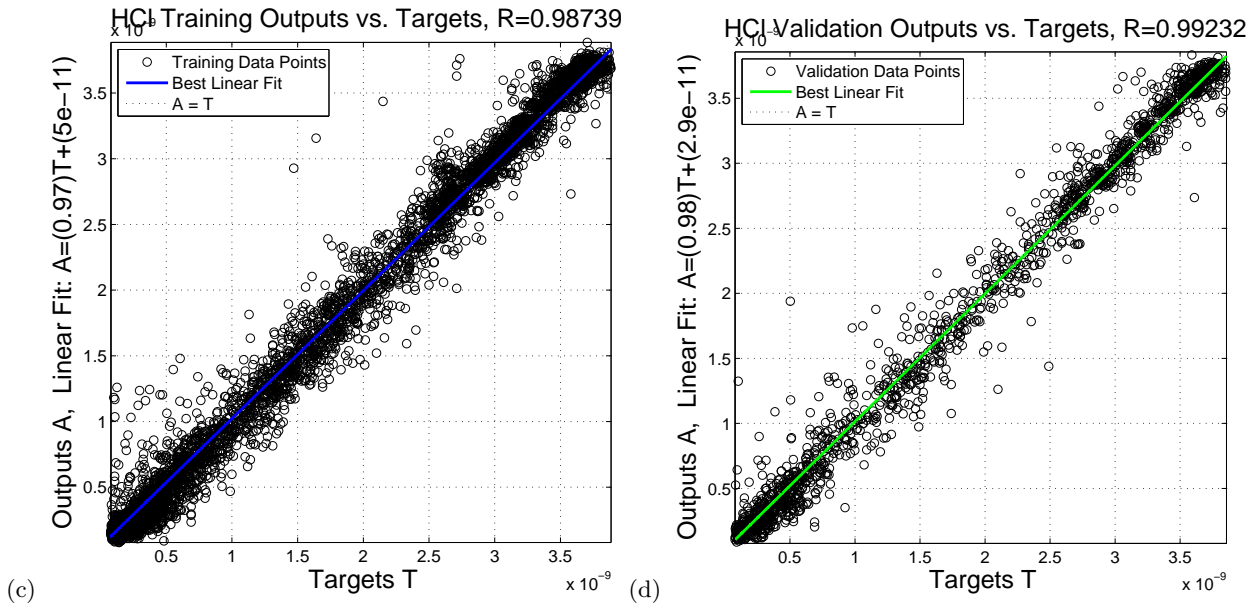


Figure 5. The panels on the left show the results of training a neural network to learn the inter-instrument biases. The panels on the right show an independent validation of this training using a randomly chosen, totally independent, data sample *not* used in training the neural network. In each case, the x-axis shows the actual ACE v2.2 HCl (the target). In panels (a) and (b) the y-axis is the neural network estimate of ACE v2.2 HCl based on MLS Aura v01 HCl. Panel (a) is the results using the training data, panel (b) is the results of the independent validation. In panels (c) and (d) the y-axis is the neural network estimate of ACE v2.2 HCl based on HALOE v19 HCl. Panel (c) is the results using the training data, panel (d) is the results of the independent validation.

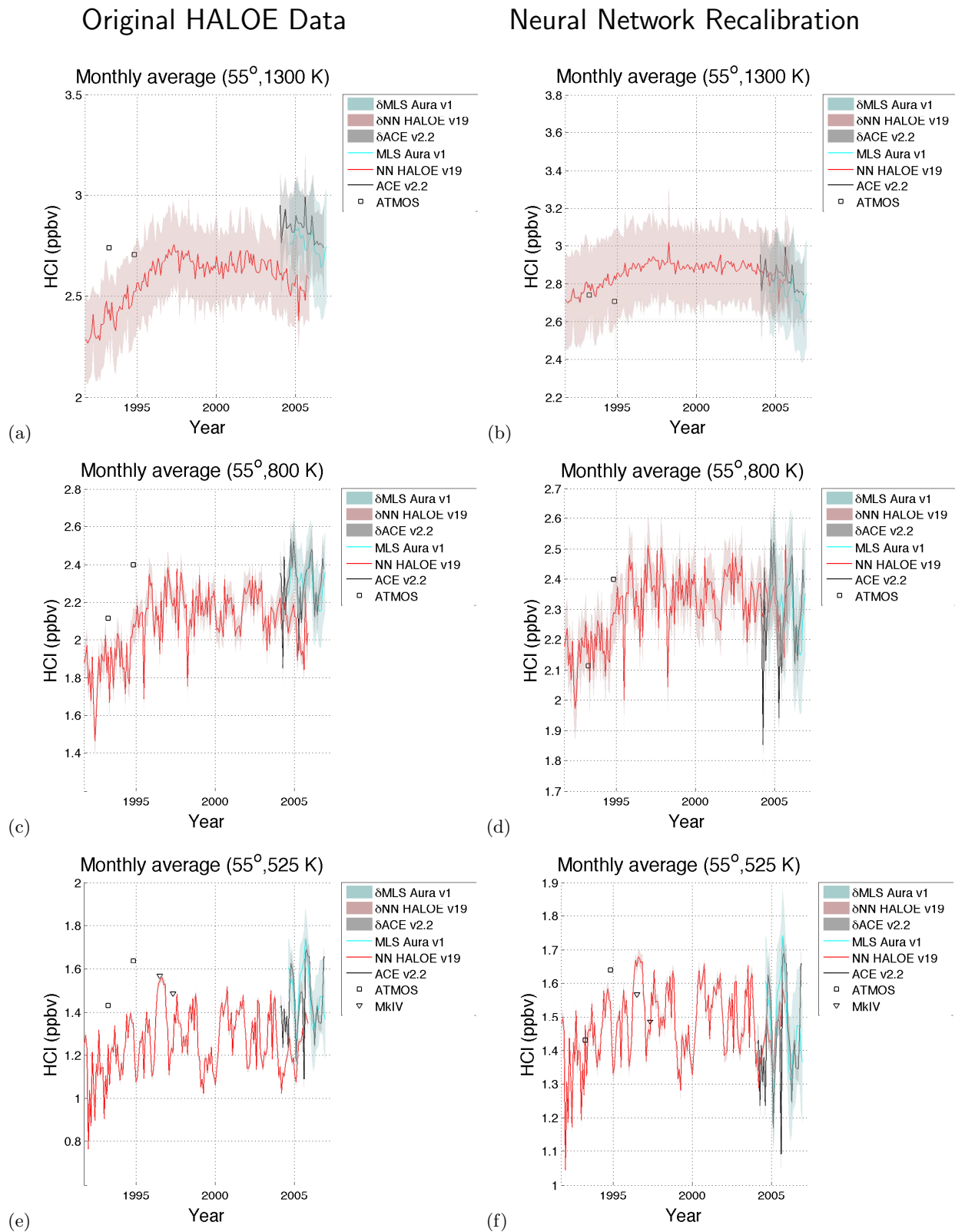


Figure 6. This figure shows HCl time-series for 55°N for three isentropic levels (525 K \approx 21 km, 800 K \approx 30 km, 1300 K \approx 41 km) from the launch of UARS to the present with HCl observations from HALOE, ATMOS, CRISTA, ACE and Aura. The panels on the left use the original v19 HALOE data. The panels on the right use the HALOE data re-calibrated with a neural network to agree with ACE v2.2 HCl.